Colloidal brushes in complex solutions: Existence of a weak midrange attraction due to excluded-volume effects

Alberto Striolo*
School of Chemical Biological and Materials Engineering, The University of Oklahoma, Norman, Oklahoma 73019, USA
(Received 6 June 2006; published 13 October 2006)

Towards the prediction of thermodynamic properties for complex systems and the design of self-assembly techniques for the production of nanocomposite materials, we employ Monte Carlo simulations to calculate the effective interactions between colloidal brushes dissolved in nonadsorbing polymer solutions. For simplicity, all interactions are reduced to excluded-volume potentials. Our results indicate that (1) due to excluded-volume effects and the absence of attractive van der Waals forces in our calculations, the effective interactions between colloidal brushes in a continuum medium are always repulsive; and (2) that the short-ranged repulsion between the colloidal brushes may be coupled to a midrange attraction when nonadsorbing polymers are in solution. We prove that a depletion mechanism is responsible for the midranged attraction and we observe that the strength of the induced attraction is weaker compared to the depletion attraction computed for hard-sphere colloids in nonadsorbing polymer solutions. More interestingly, however, our results indicate that, even for the simple interaction potentials employed here, it is not possible to superimpose depletion attraction and steric repulsion to predict the correct pair potential between colloidal brushes in nonadsorbing polymer solutions.

DOI: 10.1103/PhysRevE.74.041401 PACS number(s): 47.57.−s, 02.70.−c

I. INTRODUCTION

As a consequence of the impetus in nanotechnology research, several nanoscale building blocks are now available (e.g., icosahedral virus particles [1], thermal responsive gold nanoparticles [2], polyhedral oligomeric silsesquioxanes [3], colloidal particles with well-determined geometrical shapes [4], catalytic platinum nanoparticles immobilized on spherical polyelectrolyte brushes [5], photoswitchable colloidal brushes [6], etc.) The next challenge consists in tuning the interactions between these, and others, nanoscale building blocks to design nanostructured materials [7]. For example, under optimal conditions alkylphenylglucopyranosides form nanotubes [8] due to a combination of hydrophobic and hydrogen-bonding interactions [9] and by tuning the interactions between carbon nanotubes and polymer chains it may be possible to assemble carbon nanotube-polymer composites films [10].

The investigation of self-assembly strategies in nanotechnology builds upon the results obtained for effective particle-particle interactions in complex systems [11]. Under this perspective, mixtures of colloids and polymers provide an important class of advanced materials characterized by a wide range of mechanical, adhesive, and optical properties.

Equilibrium (e.g., stability, ordering, and adsorption) as well as hydrodynamic properties, (e.g., viscosity and friction) in complex systems are governed to a large extent by particle-particle effective interactions [12]. Colloidal particles in a solvent usually attract each other because of dispersive van der Waals forces. The effective pair interactions depend on the shape of the particles and on the chemical composition of both the colloidal particles and the intervening solvent [13,14]. In addition to dispersive attractions, electrostatic repulsions arise between like-charged particles [15], and the solvent determines important phenomena such as depletion attractions [16], solvation forces [17], and steric repulsions [18]. One of the most effective methods to stabilize colloidal suspensions is the steric stabilization obtained by end-grafting polymer chains on the particle surfaces to yield colloidal brushes [19].

While the qualitative effects on particle-particle interactions of each of the phenomena listed above are generally understood [20], the design of precise self-assembly strategies for nanotechnological applications requires the quantitative prediction of the effective interactions as a function of well-controlled experimental parameters (in the case of colloidal brushes these parameters could be the concentration of nonadsorbing polymers in solution, the density of grafted chains, etc.)

Molecular simulation techniques, especially when combined with appropriate experimental investigations, are helpful in quantifying these interactions. Here we employ Monte Carlo simulations (MC) to investigate the effective interactions between colloidal brushes in solutions containing nonadsorbing polymers. This effort continues our previous studies on the interactions between hard-sphere colloids in nonadsorbing polymer solutions [21]. We are now interested in understanding if the effective interactions between spherical colloidal particles could be manipulated by tuning entropic effects (e.g., the concentration of free polymers in solution or the density of grafted chains). To this end we do not consider any interaction other than excluded-volume effects. Our interest stems from recent experimental evidence which, in agreement with mean field theory, indicates that the layer thickness of a polymer brush on a colloidal surface increases as the surface coverage increases [22]. Under good-solvent conditions for the polymers long-range repulsive forces of osmotic origin keep the colloids apart and entropic effects restrict the interpenetration between opposing polymer chains to a narrow interfacial zone [23].

*Author to whom correspondence should be addressed. Email address: astriolo@ou.edu

Earlier theoretical studies relevant to our project concentrated on the interactions between flat surfaces covered by polymer brushes [24]. Those results could be extended to spherical particles by using the Derjaguin approximation [25]. Only recently theoreticians have explicitly considered the spherical shape of colloidal particles [26]. Roan [27], using self-consistent field theories, predicted weak attractions between colloidal brushes under specific conditions. Cerdà *et al.* [28], using MC simulations, showed that strong repulsive interactions arise between colloidal brushes depending on the density of the polymer brushes and that the force profiles follow the theory of Witten and Pincus at short colloid-colloid separations [29] and that of Flory for dilute polymer solutions at large separations [30]. Matsen [31], using the strong-stretching theory of Milner, Witten, and Cates [32], showed that the tilt angle of the grafted chains depends on the distance between two approaching colloidal brushes.

Complementing previous theoretical efforts, the results shown below demonstrate that the effective interaction between colloidal brushes in a continuum medium is always repulsive. Additionally, and more interestingly, our simulations show that it is possible to induce an effective midrange attraction between the colloidal brushes by adding nonadsorbing polymers to the solution, although the attraction is weaker than the depletion attraction observed for hard-sphere colloids dissolved in nonadsorbing polymer solutions [21,33,34]. We quantify the effective colloid-colloid interactions as a function of volume fraction of the nonadsorbing polymers in solution, density of the grafted chains, and radius of gyration of both the nonadsorbing polymers and the grafted chains. Our simulations are restricted to colloidal brushes (the chains grafted on one colloid interact with each other) dissolved in dilute nonadsorbing polymer solutions. Our results will be useful to improve existing theories which predict effective interactions between polyelectrolyte brush-coated colloids by considering the equilibrium distribution of electrolytes, but neglecting steric effects due to the presence of the brushes [35]; they can also be used to explain the face-centered cubic crystal structures that silica particles grafted with concentrated polymer brushes form in liquid suspensions [36].

This paper is organized as follows: in Sec. II we present the simulation details; in Sec. III we discuss the results obtained in this work; in Sec. IV we summarize our main conclusions.

II. SIMULATION DETAILS

We conduct our simulation calculations in the canonical ensemble (*NVT*) in which the number of particles (*N*), the volume of the simulation box (*V*), and the temperature of the system (*T*) are maintained constant [37]. All interactions are reduced to hard-sphere potentials, thus the systems investigated are at athermal conditions. Because we insert in the cubic simulation box two colloidal brushes and many nonadsorbing polymer chains, the results for the colloid-colloid effective interactions should be considered at "infinitely-dilute" concentration.

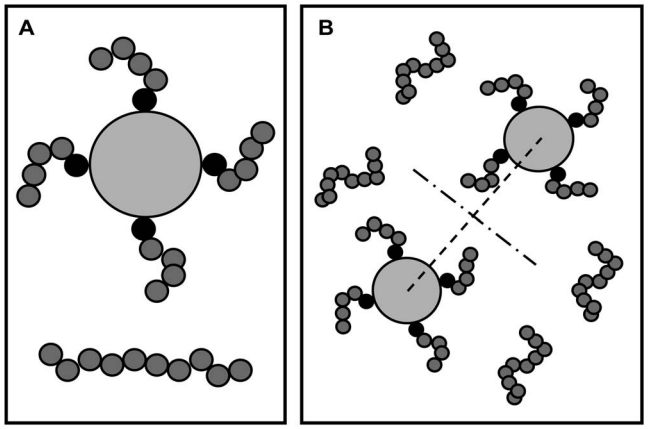

FIG. 1. Schematic representation of the systems considered in this work. In (a) we report one colloidal brush (top) and one 10-segment-long polymer (bottom). The colloidal brush in (a) is composed by one large hard sphere (light gray) and four 5-segment-long grafted chains. The black small spheres are rigidly attached to the large colloidal particles. In (b) we represent a simulation box in which 2 colloidal brushes and 4 polymers are dissolved. The dashed and dash-dot lines indicate the directions of the planes (parallel and perpendicular to the line connecting the centers of the colloids, respectively) on which we compute polymer-segment densities.

In Fig. 1(a) we report a schematic representation of one colloidal brush with four 5-segment-long side chains and of one 10-segment-long polymer. One colloidal brush is represented as one large hard sphere on which short polymer chains are grafted. The diameter of the large hard sphere equals five times the diameter of one polymer segment. The grafted chains are equally spaced on the surface of the large hard-sphere colloidal particles and modeled as freely-jointed-tangent-hard-sphere chains.

The nonadsorbing polymers in solution are modeled as freely-jointed-tangent-hard-sphere chains. The diameter of one polymer segment equals the distance between two consecutive segments in the chain and it is considered as the unit length throughout this manuscript. The simulations discussed below are conducted at dilute conditions for the nonadsorbing polymers.

To obtain the initial configuration we first place two hard-sphere colloids with no grafted chains within the simulation box at a fixed center-to-center separation. We then grow the grafted chains and, subsequently, the nonadsorbing polymers following an algorithm developed previously [21,38].

The attempted MC moves are translations and rotations. Translations are attempted for the colloidal brushes and the nonadsorbing polymers. One maximum translation vector is employed to displace the colloidal brushes, and a different one is employed to displace the nonadsorbing polymers. Both maximum translation vectors are automatically adjusted during the course of the simulation to ensure an acceptance probability of ~35%. Rotations are performed using the Pivot algorithm [39]. We attempt rotations of the entire colloidal brushes, of single grafted chains, and of the nonadsorbing polymers. The MC moves are accepted or

rejected according to the Metropolis criterion [37]. Each system is equilibrated for 20 million MC moves and the production run lasts up to 10 billion MC moves. During the production phase we sample the radial distribution function (RDF) between the centers of the colloidal brushes. From the RDF we obtain the effective pair potential of mean force (PMF) between the interacting colloids using standard statistical mechanics derivations [40]

$$\frac{W(r)}{kT} = -\ln[g(r)]. \quad (1)$$

In Eq. (1) $W(r)$ and $g(r)$ are respectively the potential of mean force and the radial distribution function at a separation r between the centers of mass of two colloidal brushes; k is the Boltzmann constant and T is the absolute temperature. From the potential of mean force it is possible to obtain the excess thermodynamic properties for the system of interest (see, for example, Refs. [41,42]).

In applying Eq. (1) we assume that the center of the large hard sphere in one colloidal brush corresponds to the center of mass of the colloidal particle. Because the grafted chains are distributed symmetrically around each colloidal sphere, this approximation should not introduce noticeable errors, especially when one assumes that the mass of the hard-sphere colloidal particle is significantly larger than that of the grafted chains. This assumption holds true in most experimental situations.

The grafted chains radii of gyration are computed by initiating separate simulation calculations in which only one colloidal brush is present within the system. The center of the colloidal brush is maintained fixed at the center of the simulation box. Attempted MC moves are translations and rotations of the nonadsorbing polymers as well as rotations of both the entire colloidal brush and the individual grafted chains. Data presented here for the grafted chains radii of gyration and for the polymer-segment density around one colloidal brush are obtained after an equilibration phase of at least 10 million MC trial moves. The production phase lasts at least 100 million MC trial moves. The radius of gyration for the nonadsorbing polymers in solutions is obtained from data available for freely-jointed-tangent-hard-sphere polymers at infinitely-dilute concentration [43]. To compute the polymer-segment density around pairs of interacting colloidal brushes we maintain the two colloids at a fixed separation and we compute the density in the two planes represented schematically in Fig. 1(b). One plane contains the line connecting the centers of both colloids and the second is perpendicular to the first line and passes through the midpoint between the two colloids.

The properties of polymer chains grafted on a surface are governed by the interactions between segments of neighboring chains. When the distance between individual grafted chains is significantly larger than their radius of gyration, freely-jointed-tangent-hard-sphere chains such as those considered here are isolated and their behavior is described in terms of the "mushroom" regime. When the distance between the grafted chains is less than their radius of gyration, they interact and stretch away from the surface. In this latter case their behavior is described in terms of the "brush" regime [44]. The properties of grafted chains in the mushroom regime are similar to those of polymers at dilute solution conditions, while those of grafted chains in the brush regime are different compared to those of polymers in solution, and depend on the shape of the surface. Theories have been developed for grafted chains in the brush regime at good-solvent conditions [19,32,45,46]. To assess the regime to which the grafted chains considered here belong to we compute their radius of gyration and we compare it to that of freely-jointed-tangent-hard-sphere chains at infinitely-dilute conditions [43]. In Fig. 2 (right) we report the ratio between the radius of gyration squared of the grafted chains to that of the chains in solution as a function of the number of the grafted chains. The grafted chains are composed of 15 (diamonds), 30 (squares), 50 (triangles), and 60 segments (circles). In all cases, the radius of gyration for the grafted chains is larger than that of the free polymer, and it increases as the number of grafted chains increases. This suggests that the grafted chains are in the brush regime in all cases considered in this work. To corroborate this result we report in Fig. 2 (left) representative simulation snapshots for colloidal brushes with 14 grafted chains of 60 segments (top), 6 grafted chains of 15 segments (center), and 20 grafted chains with 5 segments (bottom). Visual inspection demonstrates that the grafted chains interact with each other, although the interaction is clearly more pronounced for the longest grafted chains considered (top).

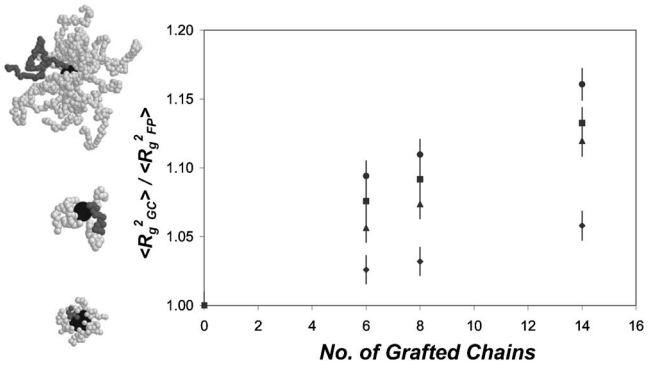

FIG. 2. Left: Representative simulation snapshots for colloidal brushes composed of 14 grafted chains of 60 segments (top), 6 grafted chains of 15 segments (center), and 20 grafted chains of 5 segments (bottom). For visualization purposes one grafted chain per colloidal brush has been colored in dark gray. Right: Ratio between the radius of gyration squared for the grafted chains ($\langle R^2_{gSC}\rangle$) and that of polymers of the same length but at infinite dilution ($\langle R^2_{gFP}\rangle$). These latter values are estimated from Ref. [43], and correspond to ~5, 12, 24, and 29 for polymers of 15, 30, 50, and 60 segments, respectively. Diamonds are for grafted chains of 15 segments, squares of 30 segments, triangles of 50, and circles of 60.

III. RESULTS

A. Colloidal brushes dissolved in a continuum medium

We first consider colloidal brushes dissolved in a continuum medium with no polymers. In Fig. 3 we report the

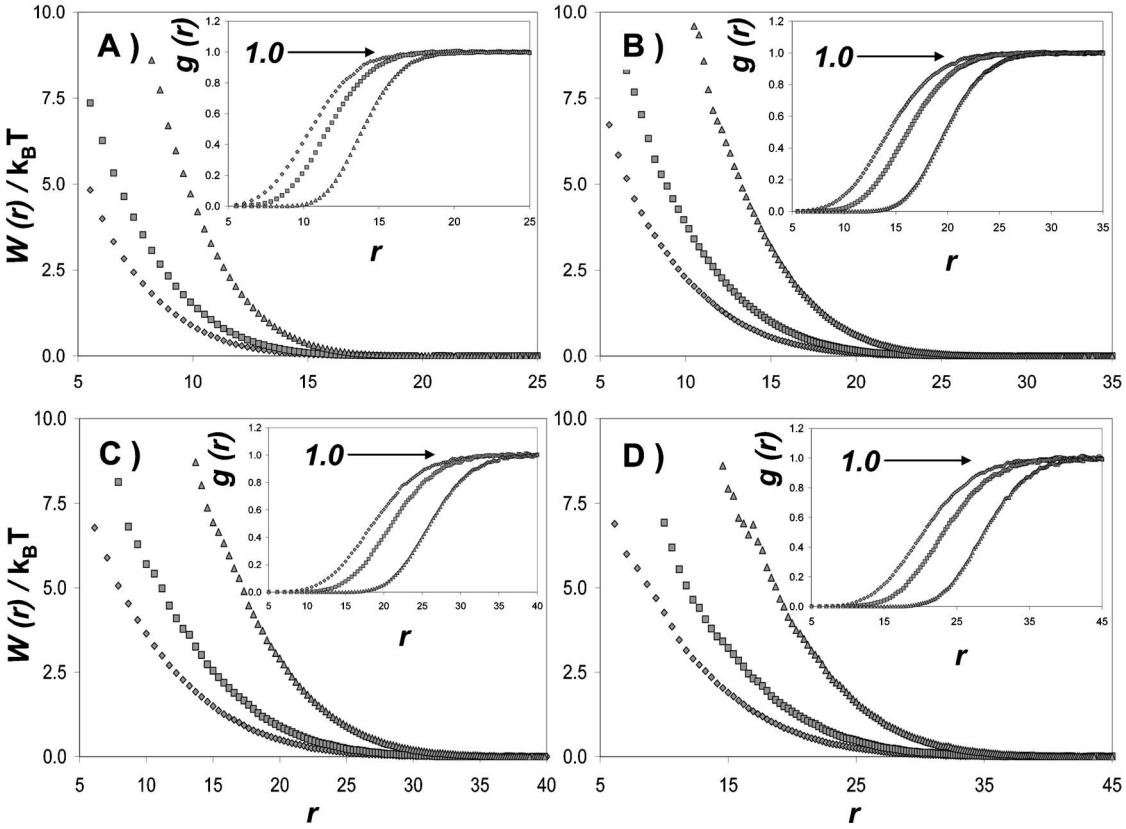

FIG. 3. Potential of mean force, $W(r)$, and radial distribution function, $g(r)$, (inset) between two colloidal brushes as a function of the number of grafted chains from MC simulations. Diamonds are for 6 grafted chains, squares for 8, and triangles for 14. The results are obtained for colloidal brushes with grafted chains of different lengths. Panel *A* is for grafted chains of 15 segments; panel *B* for grafted chains of 30 segments; panel *C* for grafted chains of 50 segments, and panel *D* for grafted chains of 60 segments. Symbols are larger than statistical uncertainty.

PMF, and the corresponding RDF (inset), between two interacting colloidal brushes. In each panel we present the results obtained for colloidal brushes with grafted chains of the same length. Panel *A* is for grafted chains of 15 segments, panel *B* for grafted chains of 30 segments, panel *C* for grafted chains of 50 segments, and panel *D* for grafted chains of 60 segments. In each panel we compare results obtained when 6 (diamonds), 8 (squares), or 14 (triangles) chains are grafted to each colloidal brush. We observe that the PMF is repulsive at all separations, in qualitative agreement with the results reported by Cerdà *et al.*. [28] for the effective interactions between colloidal brushes with 5 or 25 grafted chains. As the number of grafted chains increases, the repulsion becomes longer-ranged (because the grafted chains stretch due to crowding at the colloidal surfaces [22], see Fig. 2) and steeper (because as the number of grafted chains increases the crown of polymer segments that surrounds each colloidal particle becomes less compressible). The effective colloid-colloid repulsion observed in all the results reported in Fig. 3 is due to entropic effects originated by the presence of the grafted chains. Towards the development of accurate thermodynamic models [47] it helps observing that when the hard-sphere colloids are decorated with grafted chains (colloidal brushes), the effective pair interactions resemble those between "soft" spheres. The fewer and the longer the grafted chains are, the softer the colloidal-brush spheres become. It is also important to note that the range of the effective colloid-colloid repulsive interaction increases as the length of the grafted chains increases.

In Fig. 4 we reorganize the results presented in Fig. 3 to emphasize the effect of grafted-chain length on the colloid-colloid effective pair potentials. We only consider the PMF and the RDF (inset) between colloidal brushes with 6 (panel *A*) and 14 grafted chains (panel *B*). The length of the grafted chains is 15 (diamonds), 30 (squares), 50 (triangles), and 60 segments (circles). As observed above (see Fig. 3), the effective interactions between the colloidal brushes are repulsive at all separations. Additionally, the results shown in Fig. 4 indicate that two phenomena occur as the grafted-chain length increases. The first phenomenon is related to the range of interaction. As the length of the grafted chains increases, the effective interactions become longer ranged. This is clearly due to the fact that longer grafted chains extend towards the continuum solvent to a larger extent than short grafted chains do, thus the grafted chains of two interacting colloids "overlap" with each other at larger colloid-colloid center-to-center separations. The range of colloid-colloid repulsive interaction is of the order of four times the radius of gyration of the grafted chains. The second phenomenon is related to the steepness of the repulsive interaction. As the length of the grafted chains increases, the PMF profiles increase more gradually as the center-to-center separation

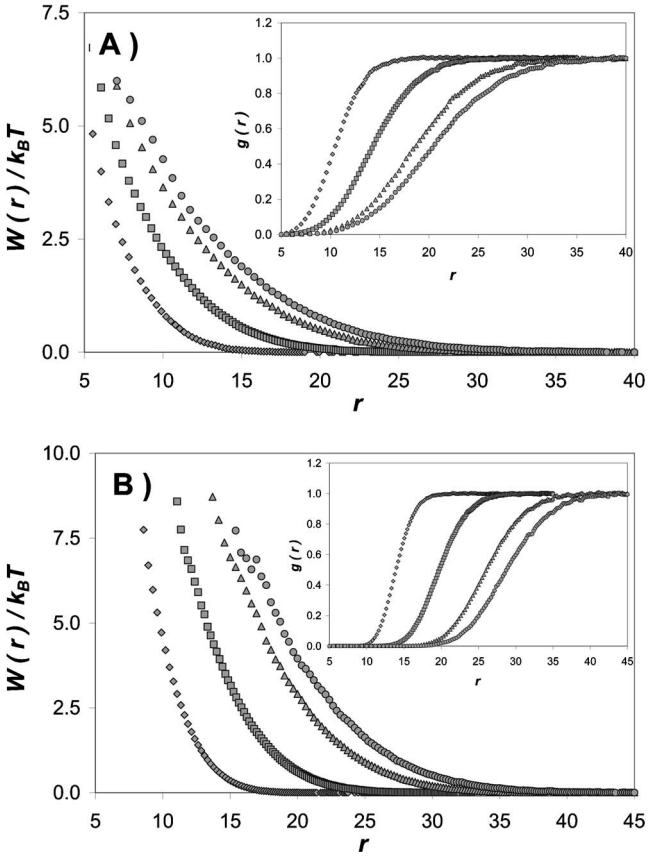

FIG. 4. PMF and RDF (inset) between two colloidal brushes as a function of the length of the grafted chains from MC simulations. The colloidal brushes have 6 (panel *A*) or 14 grafted chains (panel *B*). Diamonds, squares, triangles, and circles are for grafted chains of 15, 30, 50, and 60 segments, respectively. Symbols are larger than statistical uncertainty.

decreases, indicating that the colloidal brushes become "softer" as the grafted-chain length increases. This is probably a consequence of the spherical nature of the colloidal brushes considered here. As the length of the grafted chains increases, the grafted chains are projected further into the bulk solution, and consequently the density of polymer segments in correspondence of the end of the brush decreases (see Fig. 2). The lower the density of the grafted-chain segments is, the weaker the effective repulsion becomes because the latter is due exclusively to entropic effects.

As a special case for the results discussed in Fig. 4 we report in Fig. 5 the PMF and the RDF (inset) between colloidal brushes with 1 grafted chain. The interest in this specific system stems from two reasons: (1) recent theoretical calculations predict that in some circumstances the effective interactions between colloidal brushes with only 1 grafted chain can be attractive [27]; and (2) by concentrating the grafted chains in specific regions of the colloidal brushes we may induce directional interactions between them, thus promoting the formation of duplets, triplets, and maybe colloidal wires [4]. The length of the grafted chain in the colloidal brushes considered in Fig. 5 is 10 (diamonds), 25 (squares), 50 (triangles), and 75 segments (circles). The results obtained for the longest grafted chain show a ragged profile.

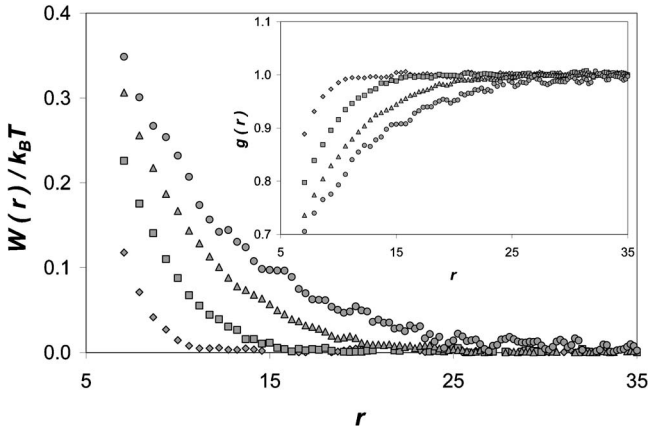

FIG. 5. PMF and RDF (inset) between two colloidal brushes as a function of the length of the grafted chains from MC simulations. The colloidal brushes have 1 grafted chain of length 10 (diamonds), 25 (squares), 50 (triangles), and 75 segments (circles). Symbols are larger than statistical uncertainty.

This is due to statistical inaccuracy observed when the simulated system becomes too dense. Our results indicate that the effective pair potentials between the two colloidal brushes are repulsive at all separations even when the grafted chain is only 10-segment long. This result disagrees with recent calculations by Roan [27], but it agrees with the general assumption that as one colloidal brush approaches another, the number of possible conformations for each grafted chain decreases, and consequently a repulsion, primarily due to entropic effects, arises between the colloidal brushes [28]. In fact there is good evidence according to which the attraction predicted by Roan between brush-coated spheres is due to numerical inaccuracy [48]. As observed above (see Fig. 4), our results indicate that as the length of the grafted chain increases, the effective interactions become longer-ranged but increase less steeply as the center-to-center distance decreases, indicating a 'softer' behavior. The results shown in Fig. 5 are orientation-averaged potentials [49], thus they do not allow us to understand if the effective colloid-colloid interactions are directional when only 1 grafted chain is considered on the colloidal brushes. We are currently initiating follow-up studies to investigate directional colloid-colloid interactions and, possibly, the self-assembly of colloidal brushes to yield, for example, colloidal wires.

B. Colloidal brushes in nonadsorbing polymer solutions

The main goal of our study is to understand if the repulsive pair potentials between colloidal brushes in solution described above may change upon the dissolution of other species in the system. We seek to induce effective attractions by exploiting entropic effects. One possibility consists in exploiting the depletion effects observed between hard-sphere colloids in nonadsorbing polymer solutions [16,21,33]. In such systems, when two hard-sphere colloids are close to each other the polymers are excluded from the gap between the interacting colloids, thus an osmotic pressure rises that induces an effective colloid-colloid attraction. For the development of accurate thermodynamic theories, it would be

interesting to understand if in solutions containing colloidal brushes in the presence of nonadsorbing polymers the entropic repulsions described above (see Figs. 3–5) can be superimposed on depletion phenomena [16,21].

We start our investigation by dissolving hard-sphere monomers of diameter equal to that of one grafted-chain segment in a system that contains two colloidal brushes. When two hard-sphere colloidal particles are in solution with hard-sphere monomers of diameter one fifth that of the colloids, a short-ranged depletion attraction is coupled to a weak midrange repulsion which is due to packing effects [50]. If the steric repulsions found between colloidal brushes (see Figs. 3–5) can be superimposed on these depletion forces the effective pair potential simulated between two colloidal brushes in the presence of hard-sphere monomers should show a weaker repulsion at close colloid-colloid separation and a stronger repulsion at midrange separations, when compared to the results obtained when the same colloidal brushes are dissolved in continuum media. We expect that the presence of a small amount of monomers in solution yields more noticeable effects when the colloidal brushes are decorated with only a few short grafted chains. However, when we consider the potential of mean force between two colloidal brushes with 6 grafted chains of 15 segments, each dissolved in a solution containing hard-sphere monomers with volume fraction 0.0055, our data (not shown for brevity) indicate that the presence of the nonadsorbing monomers does not affect appreciably the effective pair potential between the colloidal brushes. In particular, at close colloid-colloid separations the effective pair potential does not become less repulsive, neither does it become more repulsive at intermediate separations. It is possible that the volume fraction of the nonadsorbing hard-sphere monomers in solution (0.0055) is too low to generate appreciable effects on the simulated pair potential, but it is also possible, and in our opinion likely, that the grafted chains repeal the nonadsorbing monomers from the interacting colloidal brushes. Consequently the presence of the nonadsorbing hard-sphere monomers is simply not affecting the pair interactions between the colloids. Finally, because the range of effective repulsive interactions induced by the grafted chains is longer than that of depletion attractions generated by the nonadsorbing monomers (which is of the order of the hard-sphere diameter), it is possible that the depletion effect is cancelled out by the strong steric repulsion between the colloidal brushes due to the grafted chains. According to this latter speculation, the depletion effect due to the presence of nonadsorbing polymers in solution should become more significant as the ratio between the radius of gyration of the nonadsorbing polymers and that of the grafted chains increases.

To test our hypothesis we dissolve two colloidal brushes in solutions that contain nonadsorbing polymers of increasing length and concentration. When we consider the RDF and the PMF between two colloidal brushes with 6 grafted chains of 15 segments each in solutions containing nonadsorbing polymers composed of 5 segments (results not shown for brevity), our data indicate that: (1) both RDF and PMF are not affected to a large extent by the presence of the short nonadsorbing polymers in solution; and (2) although weak, the effect of dissolving the nonadsorbing polymers consists in reducing the effective colloid-colloid pair repulsion, especially at midrange separations. The weakened colloid-colloid repulsion is manifested by larger RDF and lower PMF values at defined center-to-center distances.

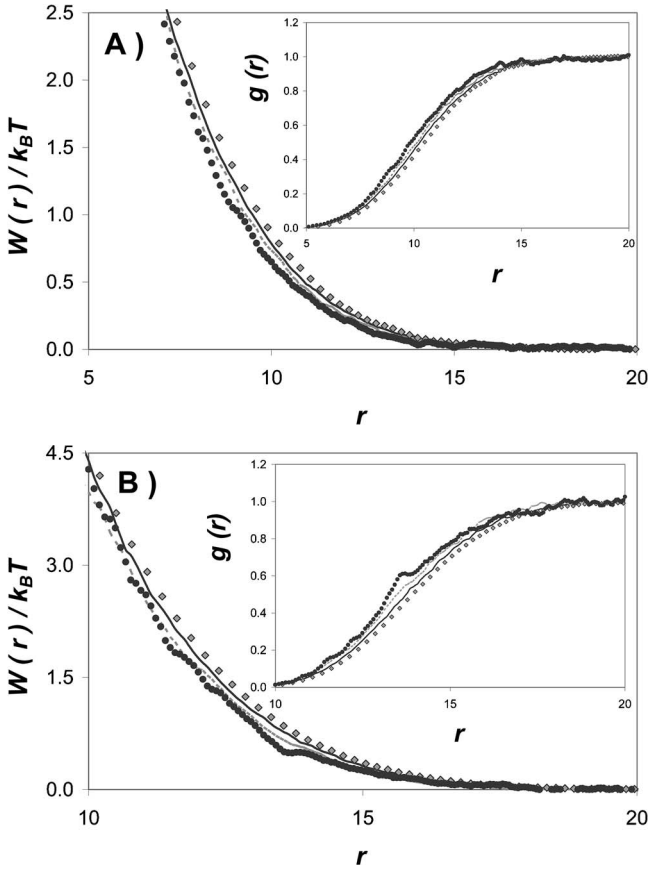

FIG. 6. PMF and RDF (inset) between two colloidal brushes with grafted chains of 15 segments dissolved in solution containing 10-segment-long nonadsorbing polymers from MC simulations. The colloids have either 6 (panel *A*) or 14 grafted chains (panel *B*). The nonadsorbing polymer-segment volume fraction is 0 (gray diamonds), 0.003 (black continuous lines), 0.006 (gray dotted lines), and 0.011 (black circles).

We expect that as the length of the nonadsorbing polymers increases, the repulsion between the colloidal brushes becomes weaker and weaker, at least at intermediate separations. In Fig. 6 we report MC simulation data for the PMF and the RDF (inset) between colloidal brushes of 6 (panel *A*) or 14 grafted chains (panel *B*). The grafted chains in the colloidal brushes in Fig. 6 are 15-segment long. The colloidal brushes are in the presence of 10-segment-long nonadsorbing polymers. Results are displayed at increasing polymer-segment volume fraction: 0 (gray diamonds), 0.003 (black continuous lines), 0.006 (gray dotted lines), and 0.011 (black circles). The statistical uncertainty increases as the polymer-segment volume fraction increases, and we believe it is responsible for the ragged data profiles obtained at the larger densities. Despite the statistical inaccuracy at large concentrations, our data indicate that the effective colloid-colloid repulsion at any colloid-colloid center-to-center

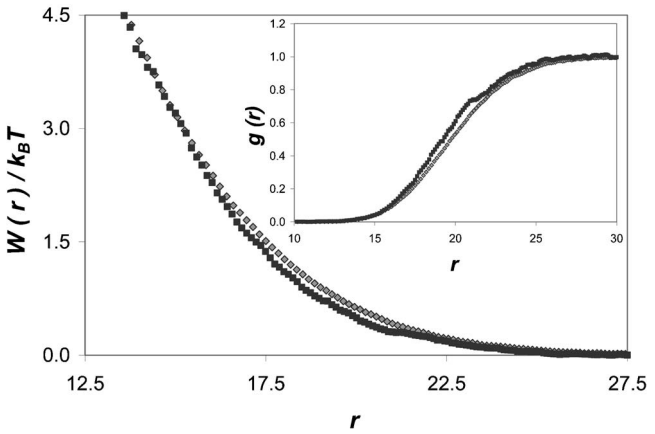

FIG. 7. PMF and RDF (inset) between two colloidal brushes with 14 grafted chains of 30 segments dissolved in solutions containing 10-segment-long nonadsorbing polymers from MC simulations. The polymer-segment volume fraction is 0 (gray diamonds) or 0.0045 (black squares). Symbols are larger than statistical uncertainty.

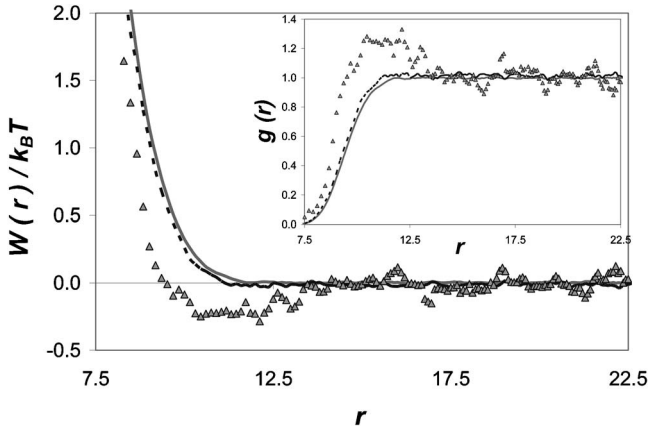

FIG. 8. PMF and RDF (inset) between two colloidal brushes from MC simulations. The colloidal brushes have 20 grafted chains, each of 5 segments. The colloidal brushes are in solution with 10-segment-long nonadsorbing polymers. The polymer-segment volume fraction is 0 (gray continuous lines), 0.004 (black dotted lines), and 0.042 (gray triangles).

separation becomes less intense as the polymer-segment volume fraction increases. Although the effect shown in Fig. 6 is more pronounced compared to that observed when shorter polymers are dissolved in the system at similar polymer-segment volume fractions, the effective colloid-colloid pair interactions remain repulsive at all the colloid-colloid center-to-center separations.

According to our hypothesis (namely that the repulsive colloid-colloid pair potential can be weakened when long nonadsorbing polymers are in solution), the effect of dissolving nonadsorbing polymers in solution on the effective colloid-colloid repulsion should become less pronounced as the length of the grafted chains increases, when the length of the nonadsorbing polymers and the polymer-segment volume fraction remain constant. In Fig. 7 we report MC simulation data for the PMF and the RDF (inset) between two colloidal brushes with 14 grafted chains of 30 segments each. The colloidal brushes are dissolved in systems that contain 10-segment-long nonadsorbing polymers. The polymer-segment volume fraction is either 0 (gray diamonds) or 0.0045 (black squares). As expected, our results indicate that, although the effective colloid-colloid repulsion becomes less intense in the presence of the nonadsorbing polymers, the effect is almost negligible. Additionally, we note that the effect is stronger at mid separations between the interacting colloids. This latter observation is quite interesting because the depletion attraction between hard-sphere colloids generated by dissolving nonadsorbing polymers in solution is stronger at short colloid-colloid separations. Further, MC simulations [21], as well as classical density-functional-theory calculations [33], predict a weak midrange repulsion between the hard-sphere colloids in the presence of nonadsorbing polymers such as those considered in Fig. 7. Thus the results shown in Fig. 7 indicate that in order to predict the effective pair potential between hard-sphere colloidal brushes dissolved in nonadsorbing polymer solutions it is not possible to simply superimpose theindependently obtained pair potentials betweenpairs ofinteracting hard-sphere colloids in nonadsorbing polymer solutions (e.g. Refs. [16,21,33]) and that between colloidal brushes in a continuum medium (e.g. Figs. 3–5).

Based on the discussion provided above, we expect that the effective pair potential between colloidal brushes could become attractive, at least at some intermediate colloid-colloid center-to-center separation, only when nonadsorbing polymers with radius of gyration longer than that of the grafted chains are present at large concentrations. To test this expectation we consider two colloidal brushes with 20 grafted chains, each composed of 5 segments, in solutions containing 10-segment-long nonadsorbing polymers. The radius of gyration squared for 10-segment-long freely-jointed-hard-sphere polymers at infinitely-dilute concentrations is ~2.9 [43], that of the grafted chains for the colloids considered in Fig. 8 is ~1.1. In Fig. 8 we display the results for the PMF and the RDF (inset) at increasing polymer-segment volume fraction. Results are shown for polymer-segment volume fraction of 0 (gray continuous lines), 0.004 (black dotted lines), and 0.042 (gray triangles). As the polymer-segment volume fraction increases from 0 to 0.004 the effective colloid-colloid pair potential becomes less repulsive at all center-to-center separations. However, the effect is minimal. When the polymer-segment volume fraction increases to 0.042 our results indicate that the strong colloid-colloid repulsion at short center-to-center separations, observed even at lower polymer-segment volume fractions, couples with a midrange colloid-colloid effective attraction of approximately 0.25 k_BT at center-to-center distances of ~10-11. This attraction is expected to become more significant as the polymer concentration increases, but computing limitations prevent us from testing this hypothesis. The midrange attraction presented in Fig. 8 is weak in absolute terms, even weaker than depletion attractions observed between hard-sphere colloids in nonadsorbing polymer solutions [21,33], but it is strong enough to promote the

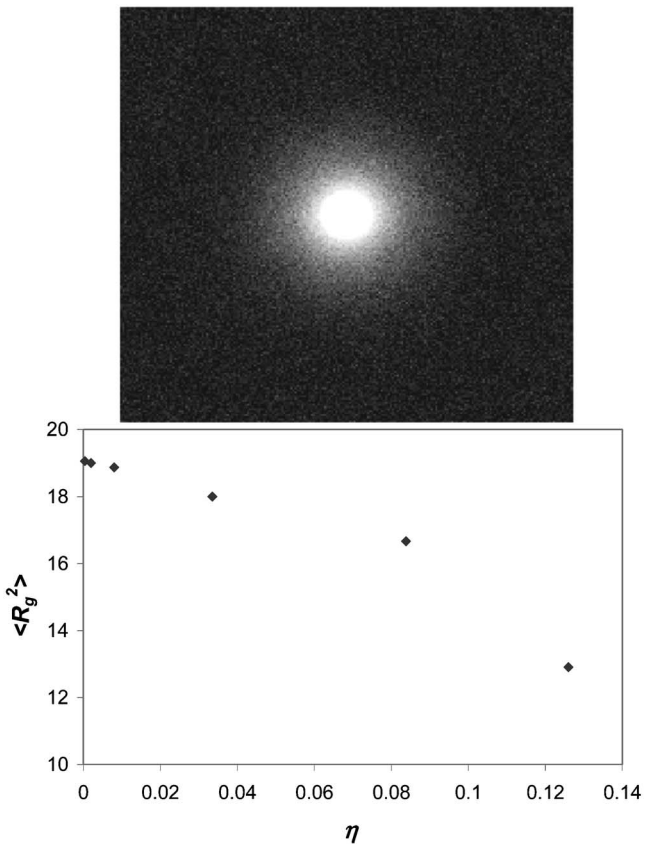

FIG. 9. Polymer-segment density around one colloidal brush (top) and radius of gyration squared of the grafted chains, $\langle R_g^2 \rangle$, as a function of the polymer-segment volume fraction, η, (bottom) from MC simulations. The colloidal brush has 8 grafted chains of 40 segments each. The top panel is obtained at polymer-segment volume fraction of 0.008. The color scheme is: black ~0.015 polymer segments per unit volume, and white ~0.002 or less.

formation of gels in colloidal systems [51], thus it could become useful for designing unique materials.

To appreciate the effect of the nonadsorbing polymers on the characteristics of the colloidal brushes we simulate one colloidal brush with 8 grafted chains of 40 segments each dissolved in a solution that contains 10-segment-long nonadsorbing polymers. This representative system was chosen because the effect of the nonadsorbing polymers on the grafted chains is expected to be more evident when few long grafted chains are on the colloidal brush. In Fig. 9 we display the density of the nonadsorbing polymer segments in a plane that passes through the center of the colloid (top) and we plot the radius of gyration squared of the grafted chains as a function of the polymer-segment volume fraction (bottom). Our results for the density of the polymer segments indicate that the grafted chains (although only 8 grafted chains are considered in the colloidal brush in Fig. 9) effectively repeal the nonadsorbing polymers from the hard-sphere colloidal particle. This phenomenon explains why to predict the exact pair potential between colloidal brushes in nonadsorbing polymer solutions it is not possible to superimpose the effective repulsion due to the chains anchored to the hard-sphere colloid and the depletion attraction due to the presence of the nonadsorbing polymers in solution. Because the grafted chains repeal the nonadsorbing polymers, the molecular mechanism responsible for the depletion attraction between hard-sphere colloids in nonadsorbing polymer solutions is not exactly reproduced in the case of colloidal brushes dissolved in nonadsorbing polymer solutions.

To further understand the effect of the nonadsorbing polymers on the isolated colloidal brushes we compute the radius of gyration squared for the grafted chains at increasing polymer-segment volume fraction (Fig. 9, bottom panel). To put our data in perspective it helps to remember that the radius of gyration squared for freely-jointed-hard-sphere polymers of 10 and 40 segments at infinitely-dilute concentrations is ~2.9 and ~17.9, respectively [43]. We note that the grafted chains radius of gyration squared is larger than that of the nonadsorbing polymers considered in this system. We also note that at low polymer-segment volume fractions the grafted chains radius of gyration squared (~19) is larger than that reported for 40-segment-long freely-jointed-hard-sphere polymers at infinitely-dilute concentrations (17.9, see Ref. [43]; see also Fig. 2). Our results suggest that the presence of the large hard-sphere colloid to which the chains are grafted, and the presence of the other grafted chains on the colloidal brush, affect the conformation of one individual grafted chain and cause it to stretch compared to its equilibrium conformation at infinitely-dilute conditions. Our results indicate that the radius of gyration of the grafted chains decreases as the polymer-segment volume fraction increases. It should be pointed out that as the polymer-segment volume fraction increases, the MC code employed in our calculations become less reliable. We do present results obtained at polymer-segment volume fraction of 0.126, but those data should only be considered as indicative. Our results imply two consequences: (1) the effective pair potential between the colloidal brushes should become shorter-ranged as the concentration of the nonadsorbing polymers increases; and (2) the effective colloid-colloid repulsion should increase faster as the center-to-center colloid-colloid separation decreases when larger concentrations of nonadsorbing polymers are in solution than when lower concentrations are. Consequently, as the nonadsorbing polymer concentration increases, the colloidal brushes will eventually behave as hard spheres of larger diameter, and at that point the depletion attraction may become observable. Although the MC simulation data presented above qualitatively support our speculations, computational limitations prevent us from verifying the latter expectation.

To understand the molecular phenomena responsible for the midrange attraction between the colloidal brushes of Fig. 8, we compute the polymer-segment density around the two interacting colloidal brushes at a fixed center-to-center separation. In Fig. 10 we report the results obtained for the polymer-segment density of the nonadsorbing polymers, that of the grafted chains, and the total polymer-segment density (nonadsorbing polymers plus grafted chains) when the colloids are at a separation of 12.5. At this separation MC simulation results suggest weak colloid-colloid attraction (see Fig. 8). Our results for the polymer-segment density (Fig. 10) indicate that the nonadsorbing polymers are repelled from

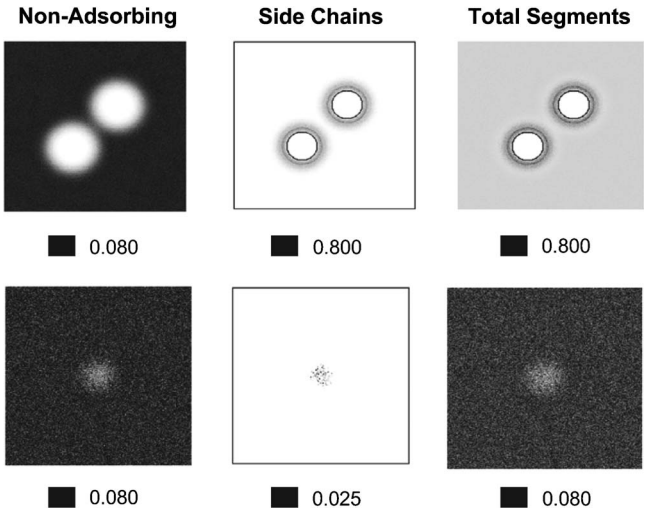

FIG. 10. Polymer-segment density around the interacting colloids maintained at a center-to-center separation of 12.5 from MC simulations. The top panels represent the results obtained in a plane through to the line connecting the centers of the colloids. The bottom panels are for the results obtained in the plane perpendicular to the line connecting the centers of the colloids. From left to right, the results are for nonadsorbing polymers, grafted chains, and total segment density (nonadsorbing polymers plus grafted chains). The color scheme is white for 0 segment density, and black for the highest segment density computed. The highest segment density changes from panel to panel, as indicated in the legend. The units are number of polymer segments per unit volume.

the interacting colloidal brushes; however we note that the total polymer-segment density is similar both in the gap between the colloidal brushes and in the region outside the colloidal brushes. Because of this, the resulting depletion attraction is weak. The grafted chains form a crown around the hard-sphere core of the colloidal brushes and effectively repeal the nonadsorbing polymers from the colloids (see Fig. 9, top panel). When we consider the plane perpendicular to the line connecting the colloids (bottom of Fig. 10) we note that a small circular region exists, in the center of the graphs, where the total polymer-segment density is less than that far from the colloidal brushes. The depletion of polymer segments from this region apparently induces the weak attraction observed in our MC calculations (see Fig. 8).

Rationalizing our results, it appears that the effective interaction between colloidal brushes is repulsive at short separations. The range of this repulsive interaction depends on the radius of gyration of the grafted chains, which increases as the density and the length of the grafted chains increase and decreases as the concentration of the nonadsorbing polymers in solution increases. This short-range repulsion can be coupled to a midrange attraction that is due to depletion effects. The range of the depletion attraction is of the order of magnitude of the radius of gyration of the nonadsorbing polymers. Because the steric repulsion due to the grafted chains is generally stronger than the depletion attraction due to the nonadsorbing polymers in solution, we speculate that it is possible to observe the midrange colloid-colloid attraction only when the radius of gyration of the nonadsorbing polymers in solution is larger than that of the chains grafted to the colloidal brush. The MC simulation results reported here support this phenomenological interpretation but clearly additional investigations are required to prove it. Due to computational limitations encountered in MC calculations, classical density functional theory provides a viable alternative route to accomplish this investigation [52].

IV. CONCLUSIONS

We employed Monte Carlo simulations to investigate the interactions between colloidal brushes in solution. We considered solutions in which the solvent was a continuum medium containing nonadsorbing polymers at dilute concentration. The molecular mechanisms operating in the systems considered in this work are limited to those of entropic origin, thus the only interactions considered are represented by excluded-volume potentials.

The effective interactions between colloidal brushes in the absence of nonadsorbing polymers are always repulsive, and the features of the potential of mean force profiles as a function of the center-to-center colloid-colloid separation depend on the number and length of the grafted chains. The range of the effective repulsion depends on the grafted chains radius of gyration. Midrange attractions between the colloids may arise when nonadsorbing polymers are present. The range of the weak attraction depends on the radius of gyration of the nonadsorbing polymers. The molecular mechanism responsible for the short-range repulsion is the steric effect due to crowding of the grafted chains in the region between the interacting colloids. The molecular mechanism responsible for the weak attraction is similar to that responsible for the depletion interaction observed between hard-sphere colloids dissolved in nonadsorbing polymer solutions. Because the short-range repulsion is always stronger than the depletion attraction (which is primarily due to the osmotic pressure of the nonadsorbing polymers in solution), it is possible to observe the midrange effective attraction between the colloidal brushes only when the radius of gyration of the grafted chains is shorter than that of the nonadsorbing polymers in solution. The resulting midrange attraction is weaker than that observed between hard-sphere colloids in nonadsorbing polymer solutions because the grafted chains in the colloidal brushes repeal the nonadsorbing polymers from the region near the interacting colloids. Our calculations prove that it is not possible to obtain the correct pair potential between colloidal brushes in nonadsorbing polymer solutions by superimposing the steric repulsion between colloidal brushes in a continuum solvent and the depletion attraction between hard-sphere colloids in nonadsorbing polymer solutions.

The results obtained with our simple model suggest that it is possible to promote the formation of novel materials (e.g., gels) by dissolving nonadsorbing polymers in colloidal systems stabilized by polymer brushes. We are currently exploring via molecular simulation possible routes to employ excluded volume effects such as those described in this paper to induce directional colloid-colloid attractions towards the production of self-assembled one-dimensional structures in solution.

ACKNOWLEDGMENTS

Partial financial support was provided by the Oklahoma State Regents for Higher Education and by the Vice President for Research at the University of Oklahoma, Norman, through a Junior Faculty Research Program award. Some calculations were performed at the Oklahoma Supercomputer Center for Education and Research (OSCER), Norman, Oklahoma. We gratefully thank Leo Lue, UMIST, for inspiring this work, and Sergei A. Egorov, UVA, for providing stimulating discussions.

[1] Q. Wang, T. Liu, L. Tang, J. E. Johnson, and M. G. Finn, Angew. Chem., Int. Ed. **41**, 450 (2002).
[2] J. Shan, J. Chen, M. Nuopponen, and H. Tenhu, Langmuir **20**, 4671 (2004).
[3] S. H. Phillips, T. S. Haddad, and S. J. Tomczak, Current Opinion in Solid State and Materials Science **8**, 21 (2004).
[4] D. Zerrouki, B. Rotenberg, S. Abramson, J. Baudry, C. Goubault, F. Leal-Calderon, D. J. Pine, and J. Bibette, Langmuir **22**, 57 (2006).
[5] Y. Mei, G. Sharma, Y. Lu, M. Ballauff, M. Drechsler, T. Irrgang, and R. Kempe, Langmuir **21**, 12229 (2005).
[6] N. S. Bell and M. Piech, Langmuir **22**, 1420 (2006).
[7] S. C. Glotzer, Science **306**, 419 (2004).
[8] J. V. Selinger, M. S. Spector, and J. M. Schnur, J. Phys. Chem. B **105**, 7157 (2001); D. Berthier, T. Buffeteau, J. -M. Leger, R. Oda, and I. Huc, J. Am. Chem. Soc. **124**, 13486 (2002).
[9] G. John, M. Mason, P. M. Ajayan, and J. S. Dordick, J. Am. Chem. Soc. **126**, 15012 (2004).
[10] P. M. Ajayan, L. S. Schadler, C. Giannaris, and A. Rubio, Adv. Mater. (Weinheim, Ger.) **12**, 750 (2000); H. D. Wagner, Chem. Phys. Lett. **361**, 57 (2002); K.-T. Lau, *ibid.* **370**, 399 (2003).
[11] D. Cao, and J. Wu, Langmuir **22**, 2712 (2006).
[12] P. Mansky, Y. Liu, E. Huang, T. P. Russell, and C. Hawker, Science **275**, 1458 (1997); M. Ornataska, S. E. Jones, R. R. Maik, M. Stone, and V. V. Tsukruk, J. Am. Chem. Soc. **125**, 12722 (2003); J. Mewis, W. J. Frith, T. A. Strivens, and W. B. Russel, AIChE J. **35**, 415 (1989); S. Neuhäusler and W. Richtering, Colloids Surf., A **97**, 39 (1995); T. Kreer, K. Binder, and M. H. Müser, Langmuir **19**, 7551 (2003).
[13] E. M. Lifshitz, Sov. Phys. JETP **2** (1956) 73; I. E. Dayaloshinskii, E. M. Lifshitz, and L. P. Pitaevskii, Adv. Phys. **10**, 165 (1961); A. J. Stone, *The Theory of Intermolecular Forces* (Oxford, UK, 1996).
[14] S. M. Gatica, M. W. Cole, and D. Velegol, Nano Lett. **5**, 169 (2005).
[15] E. J. W. Verwey and H. T. G. Overbeek, *Theory of Stability of Lyophobic Colloids* (Elsevier, Amsterdam, 1948).
[16] S. Asakura and F. Oosawa, J. Chem. Phys. **22**, 1255 (1954); A. P. Chattergee and K. S. Schweizer, *ibid.* **109**, 10464 (1998); B. Goetzelmann, R. Evans, and S. Dietrich, Phys. Rev. E **57**, 6785 (1998); R. Tuinier, G. A. Vliegenthart, and H. N. W. Lekkerkerker, J. Chem. Phys. **113**, 10768 (2000); S. Ramakrishnan, M. Fuchs, K. S. Schweizer, and C. F. Zukowski, Langmuir **18**, 1082 (2002); P. G. Bolhuis, E. J. Meijer, and A. A. Louis, Phys. Rev. Lett. **90**, 068304 (2003).
[17] R. G. Horn and J. N. Israelachvili, J. Chem. Phys. **75**, 1400 (1981); J. P. Cleveland, T. E. Shaffer, and P. K. Hansma, Phys. Rev. B **52**, R8692 (1995).
[18] C. R. Safinya, D. Roux, G. S. Smith, S. K. Sinha, P. Dimon, N. A. Clark, and A. M. Belolocq, Phys. Rev. Lett. **57**, 2718 (1996).
[19] S. Alexander, J. Phys. (France) **38**, 983 (1977); P. G. de Gennes, Macromolecules **13**, 1069 (1980); D. H. Napper, *Polymeric Stabilization of Colloidal Dispersions* (Academic, New York, 1983); E. B. Zhulina, O. V. Borisiv, and V. A. Priamitsyn, J. Colloid Interface Sci. **137**, 495 (1990).
[20] R. J. Hunter, *Foundation of Colloid Science* (Claredon, Oxford, U.K., 1987).
[21] A. Striolo, C. M. Colina, N. Elvassore, K. E. Gubbins, and L. Lue, Mol. Simul. **30**, 437 (2004).
[22] R. Hariharan and W. B. Russel, Langmuir **14**, 7104 (1998).
[23] G. H. Fredrickson and P. Pincus, Langmuir **7**, 786 (1991); G. S. Grest, Adv. Polym. Sci. **138**, 149 (1999); J. Klein, Annu. Rev. Mater. Sci. **26**, 581 (1996); X. P. Yan, S. S. Perry, M. D. Spencer, S. Pasche, S. M. De Paul, M. Textor, and M. S. Lim, Langmuir **20**, 423 (2004); M. Müller, S. Lee, H. A. Spikes, and M. D. Spencer, Tribol. Lett. **15**, 395 (2003).
[24] A. Gast and L. Leibler, Macromolecules **19**, 686 (1986); J. Mewis, W. J. Frith, T. A. Strivens, and W. B. Russel, AIChE J. **35**, 415 (1989); U. Genz, B. D'Aguanno, J. Mewis, and R. Klein, Langmuir **10**, 2206 (1994); C. M. Wijmans, E. B. Zhulina, and G. J. Fleer, Macromolecules **27**, 3238 (1994); A. P. Gast, Langmuir **12**, 4060 (1996); E. K. Lin, and A. P. Gast, Macromolecules **29**, 390 (1996).
[25] B. V. Derjaguin, Kolloid-Z. **69**, 155 (1937).
[26] C. M. Wijmans, F. A. M. Leermakers, and G. J. Fleer, Langmuir **10**, 4514 (1994).
[27] J.-R. Roan, Phys. Rev. Lett. **86**, 1027 (2001); J.-R. Roan, *ibid.* **87**, 059902 (2001).
[28] J. J. Cerdà, T. Sintes, and R. Toral, Macromolecules **36**, 1407 (2003).
[29] T. A. Witten and P. A. Pincus, Macromolecules **19**, 2509 (1986).
[30] P. J. Flory, *Principles of Polymer Chemistry* (Cornell University Press, London, 1953).
[31] M. W. Matsen, Macromolecules **38**, 4525 (2005).
[32] S. T. Miner, T. A. Witten, and M. E. Cates, Macromolecules **21**, 2610 (1988).
[33] N. Patel and S. A. Egorov, J. Chem. Phys. **121**, 4987 (2004).
[34] J. B. Hooper and K. S. Schweizer, Macromolecules **38**, 8858 (2005).
[35] H. Wang and A. R. Denton, Phys. Rev. E **70**, 041404 (2004).
[36] K. Ohno, T. Morinaga, S. Takeno, Y. Tsujii, and T. Fukuda, Macromolecules **39**, 1245 (2006).
[37] M. P. Allen and D. J. Tildesley, *Computer Simulation of Liquids* (Oxford University Press, New York, 1987).
[38] A. Striolo, D. Bratko, J. M. Prausnitz, N. Elvassore, and A. Bertucco, Fluid Phase Equilib. **183**, 341 (2001).

[39] M. Lal, Mol. Phys. **17**, 57 (1969).
[40] D. Chandler, *Introduction to Modern Statistical Mechanics* (Oxford University Press, New York, 1987).
[41] A. Striolo, J. M. Prausnitz, A. Bertucco, R. A. Kee, and M. Gauthier, Polymer **42**, 2579 (2001).
[42] F. W. Tavares, D. Bratko, A. Striolo, H. W. Blanch, and J. M. Prausnitz, J. Chem. Phys. **120**, 9859 (2004).
[43] J. Dauntenhahn and C. K. Hall, Macromolecules **27**, 5399 (1994).
[44] D. Viduna, Z. Limponchova, and K. Prochazka, J. Chem. Phys. **115**, 7309 (2001).
[45] P. G. de Gennes, Macromolecules **13**, 1069 (1980).
[46] E. B. Zhulina, O. V. Borisov, and V. A. Priamitsyn, Vysokomol. Soedin., Ser. A **31**, 185 (1989).
[47] J. M. Prausnitz, R. N. Lichtenthaler, and E. G. de Azevedo, *Molecular Thermodynamics of Fluid-Phase Equilibria*, 3rd edition (Prentice Hall, Englewood Cliffs, 1999).
[48] M. W. Matsen, Phys. Rev. Lett. **95**, 069801 (2005).
[49] D. Bratko, A. Striolo, J. Wu, H. W. Blanch, and J. M. Prausnitz, J. Phys. Chem. B **106**, 2714 (2002).
[50] R. Dickman, P. Attard, and V. Simonian, J. Chem. Phys. **107**, 205 (1997).
[51] J. Liu and E. Luijten, Phys. Rev. Lett. **93**, 247802 (2004).
[52] A. Striolo and S. A. Egorov (unpublished).